Post-print of: Wawer J., Krakowiak J., Szociński M., Lustig Z., Olszewski M., Szostak K.: Inhibition of amyloid fibril formation of hen egg white lysozyme by trimethylamine N-oxide at low pH. INTERNATIONAL JOURNAL OF BIOLOGICAL MACROMOLECULES. Vol. 70, (2014), p. 214-221. DOI: 10.1016/j.ijbiomac.2014.06.057

Inhibition of amyloid fibril formation of hen egg white lysozyme by trimethylamine N-oxide at low pH

Jarosław Wawer[a], Joanna Krakowiak [a], Michał Szociński [b], Zofia Lustig [c], Marcin Olszewski [d], Kamila Szostak [a]

[a] Department of Physical Chemistry, Faculty of Chemistry, Gdańsk University of Technology, Narutowicza Str. 11/12, 80-233 Gdańsk, Poland
[b] Department of Electrochemistry, Corrosion and Materials Engineering, Faculty of Chemistry, Gdańsk University of Technology, Narutowicza Str. 11/12, 80-233 Gdańsk, Poland
[c] Department of Chemical Technology, Faculty of Chemistry, Gdańsk University of Technology, Narutowicza Str. 11/12, 80-233 Gdańsk, Poland
[d] Department of Microbiology, Faculty of Chemistry, Gdańsk University of Technology, Narutowicza Str. 11/12, 80-233 Gdańsk, Poland

a b s t r a c t

In vitro inhibition of the formation of fibrous aggregates of proteins (amyloids) has gained increasing attention due to the number of diseases associated with protein misfolding and fibrillation. An interesting group of compounds for which pronounced activity against this phenomenon can be expected consists of low molecular weight substances (osmolytes) which have the ability to change protein stability. Here we investigate the influence of trimethylamine N-oxide (TMAO) in acidic solution (pH = 2) on the fibrillation of hen egg white lysozyme (HEWL). The process was monitored by five techniques: circular dichroism in the UV region, atomic force microscopy, dynamic light scattering, densimetry and gel electrophoresis. The obtained results show that protonated TMAO in a concentration of 400 mM inhibits amyloidogenesis. In the conditions of the experiment the HEWL molecules form clusters about 30 nm in diameter containing a relatively high fraction of covalent-bonded dimers.

Keywords: Hen egg white lysozyme, Protein aggregation, Protein dimerisation, Trimethylamine N-oxide, Amyloid inhibition

1. Introduction

Recently, studies on protein in vitro fibrillation have intensified due to their importance and have opened up new ways of investigation [1]. It has been proved that amyloids take part in the development of over 30 different disorders, including Alzheimer and Parkinson's disease. It appears that different proteins undergo a similar transformation on the way of assembling monomers into amyloid aggregates. This property seems to be an inherent feature of proteins irrespective of their primary or secondary structure [2]. What is more, even unstructured peptides (e.g. glucagon) can, in proper conditions, also form amyloid fibres [3]. All of these observations unlock new opportunities and suggest that findings regarding model systems can be confronted with systems of biological importance.

Hen egg white lysozyme (HEWL) is one of the most commonly used model proteins in this type of studies. The procedure of preparing amyloids from HEWL is well known and has been described in detail. The simplest and most widely used method is to incubate a solution of HEWL (pH = 2) in elevated temperature [1]. In the present work a similar approach was applied – acidic solutions of lysozyme (pH = 2) enriched with trimethylamine N-oxide (TMAO) were heated at 60 °C for 72 h.

Considerable effort has been paid to find an effective inhibitor of amyloidogenesis. Among the variety of tested classes of compounds which impact hen egg white lysozyme fibrillation the following are worth mentioning: ions, salts and ionic liquids [4–6], amphiphilic compounds [7,8], denaturing agents [9,10], crowding agent [11], and planar aromatic compounds [12,13]. In this study the inhibitory properties of trimethylamine N-oxide were tested. This compound is a well-known osmolyte whose hydration properties [14] and influence on the stability of HEWL were previously investigated [15,16]. According to these research studies, TMAO does not interact directly with the protein. The addition of TMAO shortens the water hydrogen bonds, what promotes tighter protein folding. As a result, thermal stability of the protein increases.

It has been suggested that partial unfolding of the protein is the first step in amyloidogenesis [17]. Therefore, it seems reasonable to implement target-oriented action and to control the entire process influencing this stage of aggregation. Changing protein stability deserves particular consideration since it may provide an easy and convenient way to modifying the rate of amyloidogenesis [18].

http://dx.doi.org/10.1016/j.ijbiomac.2014.06.057

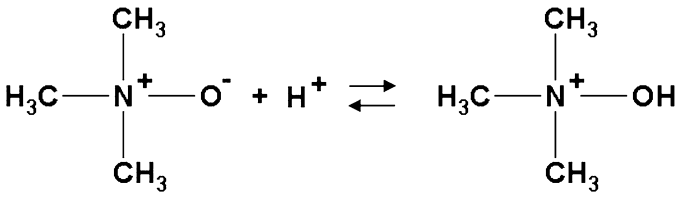

Fig. 1. Reaction of trimethylamine N-oxide (TMAO) with hydrogen ion.

The effect of osmolytes on the fibrillation of proteins was summarised in a work published by Macchi et al. [3]. An analysis of the data presented in the paper revealed that osmolytes have a different impact on the discussed phenomenon. Adding osmolytes to the reaction mixture can increase the rate of amyloid fibril formation or can inhibit aggregation. The obtained result depends on the investigated protein and on the concentration of the osmolyte. In many cases the osmolyte's presence does not affect the amyloidogenesis.

To the best of our knowledge, information on TMAO's impact on amyloid fibril formation made from HEWL is lacking. In the conditions of measurements as presented in this study (low pH), TMAO is protonated (Fig. 1) [19]. Contrary to neutral pH, trimethylamine N-oxide in acidic conditions acts as a protein destabiliser [20]. This behaviour is probably caused by the fact that the positively charged molecules of TMAO bind preferentially to HEWL and decrease the enthalpy of denaturation [20].

The main aim of this work is to explore amyloid fibril formation at its early stage. In order to prevent protein degradation (hydrolysis), the time of exposure of the protein molecules to low pH should be minimised; however, incubation should be long enough to obtain amyloids. Reaction mixtures containing a high concentration of proteins (25 mg/ml) were used to meet these requirements.

2. Materials and methods

2.1. Solution and fibrils preparation

Hen egg white lysozyme (HEWL) (Fluka, Cat. No. 62971) was dialysed against deionised water and lyophilised. The TMAO solution was prepared by dissolution of trimethylamine N-oxide (TMAO) (Fluka, ≥99.0%) in HCl solution (Chempur, pure). The pH was adjusted to 2 by the addition of HCl. The working solution was prepared by dissolution of the lysozyme in the TMAO solution to a final concentration of 25 mg/ml (determined by weight). The protein solution was filtrated twice by a 0.2 μm syringe filter. The exact protein concentration was determined spectroscopically (see below). The stock solution was stored in a refrigerator. A sample was taken every 12 h and placed into an incubator (60 °C). The experiment was terminated after 72 h and all the samples were analysed. In order to perform measurements, each sample was diluted to final concentrations (all in mg/ml): AFM: 0.3; CD: 0.15; DLS: 0.5; electrophoresis: 10; densimetry: 25.

2.2. Atomic force microscopy (AFM)

AFM scans were performed on an AFM N-Tegra Aura microscope. The non-contact working mode was used. Tip size was 10 nm and the scan frequency was equal to 0.8 Hz. Ten microlitre of the sample was applied on a freshly cleaved mica surface dried and stored in a desiccator over P_2O_5.

2.3. Dynamic light scattering (DLS)

Dynamic light scattering measurements were performed using the Malvern Zetasizer Nano ZS. The apparatus was equipped with a laser with a wavelength of 633 nm. Samples were placed into disposable cuvettes with a 1 cm optical path. Scatter radiation was collected at an angle of 173° (backscatter mode). Each scan consisted of 20 runs and the run duration was 20 s. Scans were repeated three times for every sample. The temperature of the measurements was set to 25 °C. The refractive index of the material (protein) and the absorption were set to 1.450 and 0.001, respectively. The following parameters were used for the dispersant: viscosity 0.8872 cP, refractive index 1.330. The collected data were analysed using the non-negative least squares method (NNLS).

2.4. Circular dichroism (CD)

Circular dichroism spectra in the UV region (193–260 nm) were measured on a Jasco J-815 spectropolarimeter. The scans were recorded at a speed of 50 nm/min with a step size of 0.2 nm. The optical length was equal to 1 mm. Six scans were accumulated for every sample. The samples were prepared by weighted dilution of the working solutions and the concentration was calculated from the known concentration for stock solution. Obtained spectra were interpreted with help of the K2D algorithm [21,22].

2.5. Densimetry

Densities of the TMAO solutions without the addition of protein and densities of HEWL solutions were determined using the Anton Paar DMA 5000 densimeter. All measurements were performed at 20 °C and the temperature was kept constant to ±0.001 °C. Precision of measurements and accuracy were equal to 1.0×10^{-6} and 5.0×10^{-6} g/ml, respectively.

2.6. Gel electrophoresis (SDS-PAGE)

SDS-reducing polyacrylamide gel electrophoresis was performed in a Tris–tricine buffer solution. Marker: Fermentas, SM1861. Coomassie Brilliant Blue G250 dye was used for staining.

2.7. UV absorbance spectroscopy

UV–vis absorbance spectra were recorded on a Thermo Evolution 300 spectrophotometer. The protein concentration was calculated using the extinction coefficient $\varepsilon = 2.65\ \mathrm{dm^3\ g^{-1}\ cm^{-1}}$ at $\lambda = 280$ nm. Three scans were averaged for each sample.

2.8. Statistical analysis

Uncertainties of measured values Δy were estimated using the total differential method according to the equation:

$$\Delta y = \sum \left| \frac{\partial f(x_i)}{\partial x_i} \right| \cdot \Delta x_i \qquad (1)$$

where $f(x_i)$ was the function used to calculate parameter y and Δx_i was the uncertainty of the measured quantity.

3. Results and discussion

The analysis of structural changes of protein during incubation was based on circular dichroism measurements in the UV region of the spectrum (CD-UV). Due to the low content of amyloids caused by a relatively short time of incubation, the CD-UV spectra presented as mean residue molar ellipticity versus wavelength overlap and were not particularly informative. However, useful information, i.e. estimation of the protein secondary structure, was derived from the measured data by using an artificial neural network based algorithm (K2D) [21–23]. The obtained results are presented in

Table 1
Structural changes of the HEWL during incubation at 60 °C.

Incubation time [h]	0 mM TMAO			50 mM TMAO			250 mM TMAO[a]			400 mM TMAO		
	α [%]	β [%]	Random coil [%]	α [%]	β [%]	Random coil [%]	α [%]	β [%]	Random coil [%]	α [%]	β [%]	Random coil [%]
0	33	15	51	35	15	50	33	15	52	34	15	50
12	30	15	54	30	15	55	32	15	53	34	15	50
24	27	16	56	27	16	56	29	15	56	31	15	53
36	26	17	57	25	18	57	26	17	57	30	15	54
48	24	20	56	24	19	57	26	18	56	29	15	55
60	22	22	57	23	21	56	22	22	56	29	15	56
72	20	23	57	23	22	55	22	23	55	26	15	59

[a] Concentration of the protein determined for individual samples (see below).

Table 1. For the sake of clarity, changes in the fraction of β-sheet and α-helix during heating are shown in Fig. 2.

Inspection of the data from Table 1 revealed that the content of the β-sheet and α-helix in native HEWL in unheated solution at pH = 2 equals 15% and 33–35% irrespective of the concentration of TMAO. The obtained values are in good agreement with literature data [7].

As has been shown [7], the formation of amyloids is accompanied by an increase in the fraction of β-sheet and a decrease in the α-helix content. The presented results confirmed this conclusion. An increase in the content of the β-sheet was detected for samples containing from 0 mM to 250 mM TMAO after a lag time of 24 h.

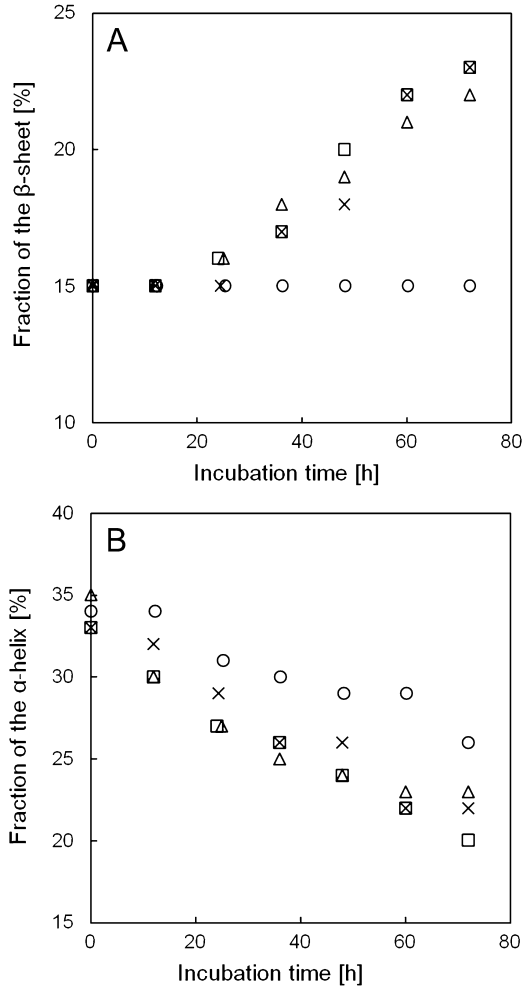

Fig. 2. Structural changes of HEWL during incubation at 60 °C obtained from circular dichroism measurements; (A) fraction of β-sheets, (B) fraction of α-helix. Concentration of TMAO: □ – 0 mM TMAO; △ – 50 mM TMAO; × – 250 mM TMAO; ○ – 400 mM TMAO.

A lag time for samples in which the concentration of TMAO was 250 mM appears to be slightly higher; however, it does not exceed 36 h. The protein in a solution of 400 mM TMAO does not undergo this transformation. In this case the percentage of the β-sheet in the secondary structure of the molecules remained constant at a level of 15%. This observation may suggest that a high concentration of TMAO in the acidic solution inhibits the assembly of HEWL into amyloid fibrils.

A monotonic decrease in the α-helix content was recorded for all samples (Fig. 2). This reduction was probably caused by ongoing irreversible denaturation of the protein. The literature data show that the midpoint of melting temperature depends on both pH and the concentration of TMAO and is close to 60 °C (from 58 °C to 54.5 °C) [20]. For samples containing a high amount of TMAO the drop in the fraction of the α-helix was remarkably less steep. This observation also supports the suggestion that a high concentration of TMAO has a significant impact on the investigated process.

The protein becomes less structured during incubation in elevated temperature. An analysis of the CD-UV spectra indicates that the fraction of random coil increases in each sample (Table 1). However, tests with a low concentration of TMAO show that after 36 h a plateau was reached (the fraction of random coil stabilised at around ~56%). The trend observed for 400 mM TMAO differed considerably. At the beginning of incubation an increase in the unstructured region was smaller but the plateau was not present. A high concentration TMAO inhibited the formation of β-sheets but did not stop protein irreversible denaturation completely, i.e. it only slowed it down.

Atomic force microscope (AFM) images for samples with a different concentration of TMAO taken after 72 h of incubation at 60 °C are shown in Fig. 3. The AFM scans correspond to generalised information gained from analysis of the CD-UV spectra. The main difference lies in the lag time obtained from CD-UV and the incubation time after which the amyloids were detected by AFM imaging. According to the AFM study, fibrils appeared after 48 h of heating in the sample without TMAO. This time length was equal to 60 and 36 h for samples with 50 and 250 mM TMAO, respectively. The discrepancies between CD-UV and the AFM scans could have been caused by two reasons. First, detection of amyloids using AFM could be difficult due to experimental problems, especially for samples where the concentration of the TMAO was high. In these conditions the formed fibrils are often accompanied by deposits of the examined additive or amorphous aggregates made of protein (Fig. 3B). In the results the tested area is covered by objects that are very different in height, which obviously make the whole process more laborious and uncertain. In that context the analysis of CD-UV spectra seems to be more sensitive and devoid of the human factor, i.e. it is more objective.

Secondly, as has been previously suggested, amyloidogenesis is preceded by the formation of various types of intermediates [2,18,24]. Alternation of the secondary structure of the protein in the fibril precursors results in CD-UV spectra transformation. It appears that in our case a significant amount of intermediates

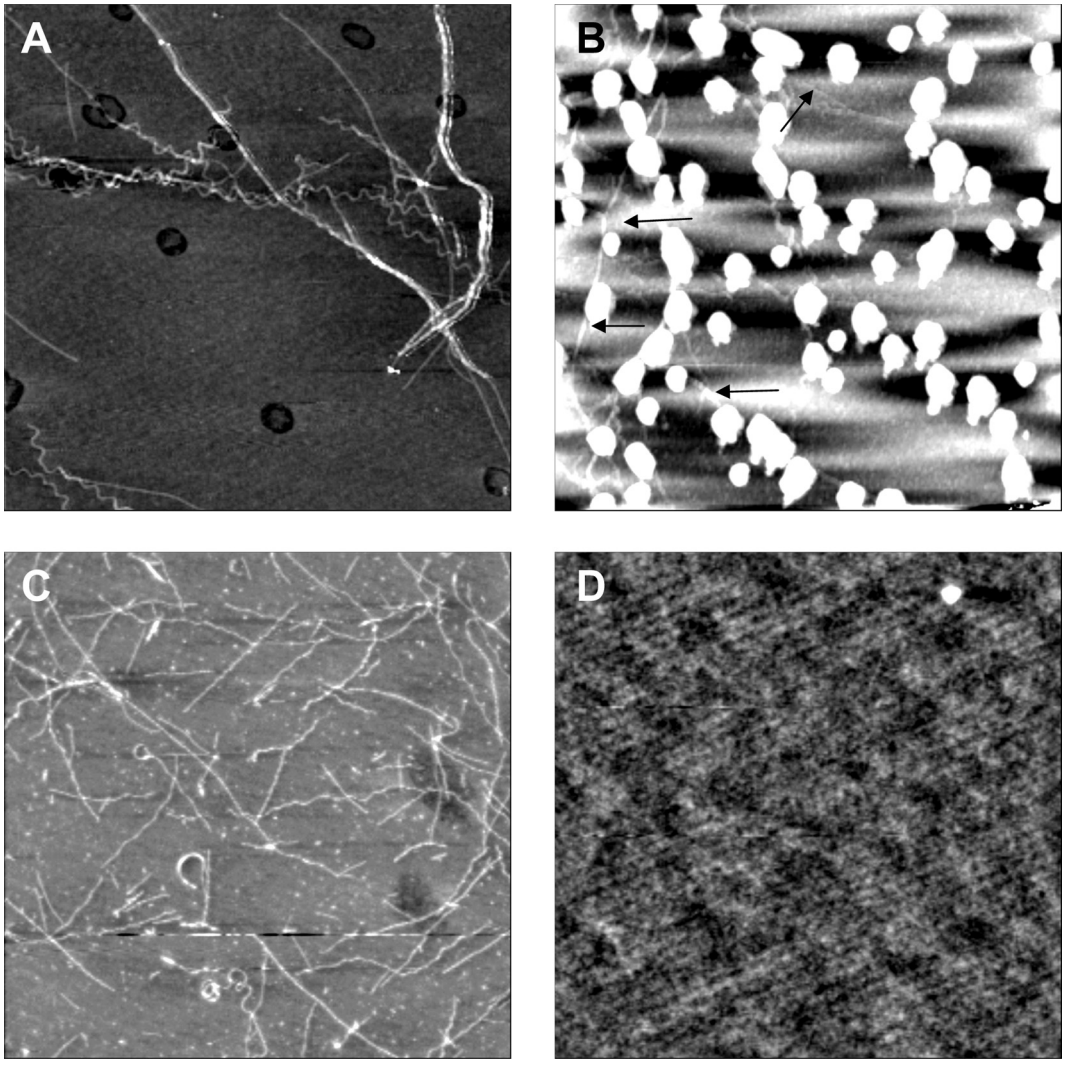

Fig. 3. Atomic force microscopy height images of fibrils formed in samples incubated at 60 °C for 72 h (10 × 10 μm). Concentration of TMAO: (A) 0 mM TMAO; (B) 50 mM TMAO; (C) 250 mM TMAO; (D) 400 mM TMAO.

was created at an early stage of amyloid fibril formation. These assembly competent intermediates did not possess mature fibril morphology, although their structure was enriched by β-sheets [6,25].

The morphology of the final form of amyloids strongly depended on the concentration of TMAO. Protofibrils made by incubation of HEWL at 60 °C for 72 h without addition of TMAO (Fig. 3A) had a sinusoidal, wavy shape. However, mature fibrils made of several of these components were straight. For the sample with 250 mM TMAO the fibrils were much shorter and did not have this distinctive, folded structure. The high concentration of TMAO inhibited the formation of amyloids completely. In this sample the surface of the mica was evenly coated with small, globular particles.

Prolonged exposure of the protein to harsh conditions may lead to undesirable reactions (mainly degradation), which are not of interest for this paper. To assess the extent of these unwanted phenomena, gel electrophoresis in denatured conditions (SDS-PAGE) was performed. The results of these tests for samples with 250 and 400 mM TMAO are presented in Fig. 4. The gels for 0 and 50 mM TMAO were virtually identical to the gel for 250 mM TMAO, thus they were not shown. The wells were slightly overloaded to observe even the smallest fraction of the products of hydrolysis. The adopted approach is a common method of evaluating the process of in vitro amyloid formation. As has been previously proved [1], amyloid fibrils are held solely by physical bonds and can be dissociated by the addition of sodium dodecyl sulfate (SDS) and heating. Since there is no covalent bond between the subunits, one can expect that the obtained bands would correspond to monomeric HEWL and the hydrolysis products. The electrophoresis gels for samples where the concentration of TMAO ranges from 0 mM to 250 mM fully confirms the correctness of this prediction. For each of these samples, apart from the bands which can be assigned to denaturated HEWL, additional bands appeared (the most intensive one was slightly above 10 kDa). The elongated time of incubation results in extended protein degradation and thus the intensity of this band increased.

Unlike for the low concentration TMAO systems, for samples with 400 mM TMAO the increase in bands assigned to dimers and other aggregates of HEWL were reported (Fig. 4B). This increase was particularly visible for samples heated longer than 36 h. Obviously, since the created complexes were not dissociated by SDS, the formed bonds must have been covalent. The repeated test (gel not shown; concentration 0, 200, 300, 400 mM TMAO) confirmed that dimerisation was significant only for the highest concentration of this osmolyte. This observation alone can be a starting point for future research. A review of the literature reveals that dimers can by produced by vacuum heating (85 °C) of the solid-state lysozyme [26–28] or by UV irradiation of the solution [29]. The experimental

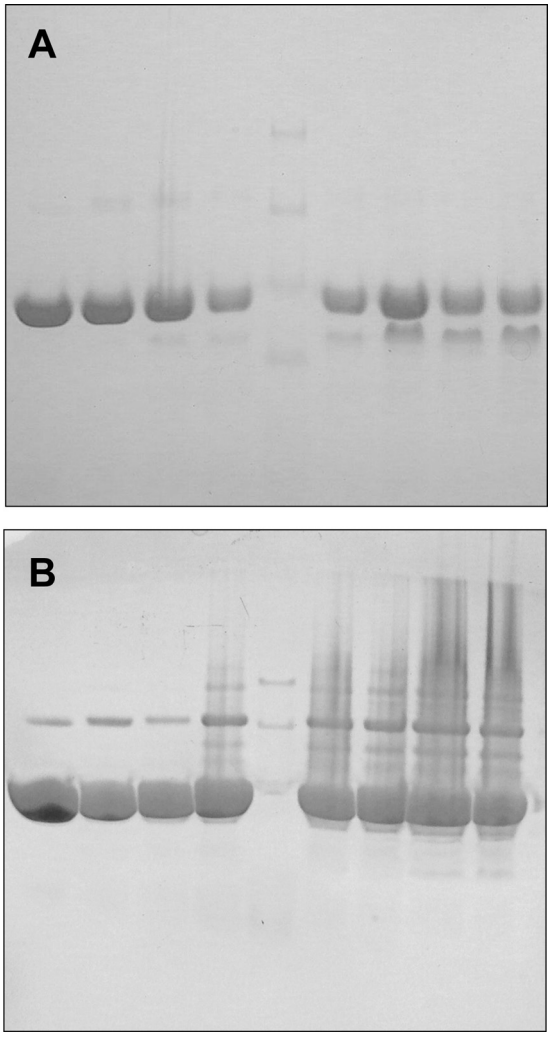

Fig. 4. SDS-PAGE gel of samples of HEWL: from left: line 1 – native HEWL; lines 2–4 and lines 6–9 incubated samples (from 0 h to 72 h); line 5 – marker (40, 25, 15, 10 kDa). Concentration of TMAO: (a) 250 mM; (b) 400 mM

conditions in this study were less drastic and thus potentially more advantageous. We plan to explore these aspects in greater detail in future works.

Ongoing aggregation and the overall changes occurring with thermal incubation may be readily monitored by measuring the specific volume of protein, V_s. The V_s value was calculated according to the following equation [30]:

$$V_s = \left(\frac{1}{w}\right) \cdot \left(\frac{1}{d} - \frac{1}{d_0}\right) + \frac{1}{d_0} \quad (2)$$

where w ($g/g_{solution}$) is the mass fraction of the protein in the solution, d (g/ml) and d_0 (g/ml) are the densities of the solution and the solvent, respectively. For each sample (except 250 mM TMAO) the concentration of the protein in the stock solution was determined spectroscopically and after appropriate recalculation was used to obtain V_s for every sample, irrespective of the heating time. For samples containing 250 mM TMAO, due to minor protein precipitation the concentration of every sample was determined separately. The obtained densities of the solutions and the solvents as well as calculated values of specific volumes of protein are collected in Tables 2 and 3.

Measurements of changes of V_s for systems without the addition of TMAO were conducted two times. First, the samples were prepared as described in Section 2.1, i.e. every 12 h the sample was

Table 2
Density of the solvent, d_0, and HEWL solutions, d, without TMAO (pH = 2). Apparent specific volumes of HEWL, V_s, after incubation at 60 °C.

Incubation time [h]	Single-day measurements		Daily measurements	
	d [g/ml]	V_s [ml/g]	d [g/ml]	V_s [ml/g]
	d_0 = 0.998421	–	d_0 = 0.998416	–
0	1.005062	0.7153	1.004965	0.7160
12	–	–	1.005013	0.7139
24	1.005087	0.7142	1.005032	0.7131
36	–	–	1.005046	0.7125
48	1.005122	0.7127	1.005057	0.7120
60	1.005134	0.7122	1.005067	0.7116
72	1.005153	0.7114	1.005102	0.7101

removed from the stock solution, which was kept in a refrigerator, and placed into an incubator. After 72 h all samples were taken out and analysed. In the second test the sample was kept in the incubator at 60 °C and measurements were repeated every 12 h. Both methods gave approximately equal values of specific volumes of protein (see Fig. 5), which proves that the applied procedure is reliable.

A proper interpretation requires splitting the V_s value into three components:

$$V_s = V_{int} + V_{ele} + V_{str} \quad (3)$$

This expression indicates that introduction of the solute possessing an intrinsic volume of V_{int} will cause electrostatic compression of water (V_{ele}) and rearrangement of the solvent (V_{str}). In the present work, however, more attention should be paid to the change of the specific volume ΔV_s which occurred during heating:

$$\Delta V_s = \Delta V_{hyd} + \Delta V_{protein} + \Delta V_{aggr} \quad (4)$$

Parameters ΔV_{hyd}, $\Delta V_{protein}$ and ΔV_{aggr} describe the change of the volume due to hydrolysis of the protein, structural change of the protein and aggregation.

With progressing hydrolysis the protein is continuously converted into oligopeptides and free amino acids. It should be noted that for amino acids from the interior of the protein the V_{int} is very important and V_{ele} and V_{str} are negligible. Exposition of these amino acids to water affects the structure of the solvent and thus the difference between the partial molar volume and its intrinsic volume becomes crucial. It seems that amino acids, despite their hydrophilic properties, have a large positive V_{str} contribution [14]

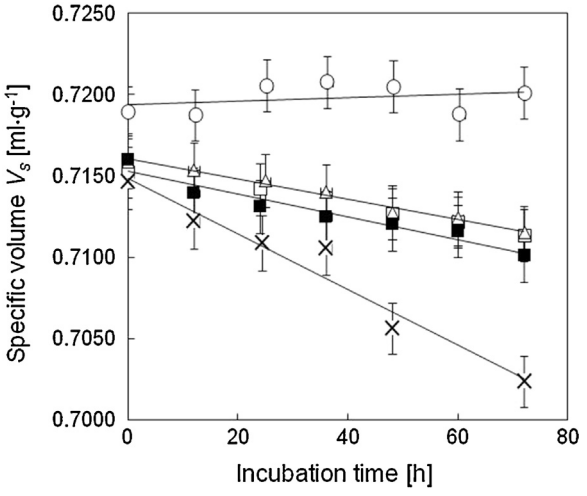

Fig. 5. Changes of the specific volumes of HEWL during incubation at 60 °C. Concentration of TMAO: □ – 0 mM TMAO (single-day measurements); ■ – 0 mM TMAO (daily measurements); △ – 50 mM TMAO; × – 250 mM TMAO; ○ – 400 mM TMAO.

Table 3
Density of the solvent, d_0, densities of the HEWL solutions, d, apparent specific volumes of HEWL, V_s, after incubation at 60 °C. The concentration of the TMAO ranging from 50 mM to 400 mM.

Incubation time [h]	50 mM TMAO		250 mM TMAO[a]		400 mM TMAO	
	d [g/ml]	V_s [ml/g]	d [g/ml]	V_s [ml/g]	d [g/ml]	V_s [ml/g]
	$d_0 = 0.999172$	–	$d_0 = 1.002383$	–	$d_0 = 1.004514$	–
0	1.005514	0.7159	1.008497	0.7146	1.010750	0.7189
12	1.005525	0.7154	1.008500	0.7122	1.010754	0.7187
24	1.005540	0.7147	1.008535	0.7109	1.010713	0.7206
36	1.005555	0.7140	1.008195	0.7106	1.010708	0.7208
48	1.005584	0.7128	1.007939	0.7056	1.010714	0.7205
60	1.005592	0.7124	–	–	1.010753	0.7188
72	1.005612	0.7115	1.007906	0.7024	1.010723	0.7201

[a] Concentration of the protein determined for individual samples (see below).

and, as a result, it can be expected that ΔV_{hyd} will also be positive. It is far more difficult to predict the sign of $\Delta V_{protein}$. It was reported that thermal denaturation leads to a small decrease in the volume [31,32], but there is no obvious clue as to how the volume of protein changes due to the formation of β-sheet enriched structures. The ΔV_{aggr} can be estimated by assuming that water molecules from the solvation sphere around monomeric HEWL are rearranged in a way that $V_{str} > 0$. The association of the protein release this solvent and thus ΔV_{aggr} is negative. The sum of the above-mentioned effects gives a negative value of ΔV_s. Similar results, i.e. a decrease in the specific volume of protein, was obtained for experiments on the amyloidogenesis of insulin [33]. The present work contradicts, however, the report on aggregation of a disulfide-deficient variant of hen lysozyme [34].

The trends of V_s against time obtained for 0 and 50 mM of TMAO overlap (Fig. 5), which proves that the low concentration of trimethylamine N-oxide has almost no impact on amyloidogenesis. The steep slope for the samples containing 250 mM of TMAO is probably an artefact of the calculation procedure and should be treated with caution. In this case the concentration in each of the incubated samples was determined using the extinction coefficient of the unheated lysozyme, which does not necessarily reflect the truth.

The specific volume of the HEWL at the highest tested concentration of TMAO remained virtually constant. This finding is consistent with suggestions that 400 mM of TMAO inhibits amyloid fibril formation. The small increase of V_s is probably the result of protein degradation which, in fact, appears to be less important than for the other samples (see Fig. 4). These observations implicate that covalent-bounded dimers and other forms of aggregates present in 400 mM TMAO samples have a negligible contribution in ΔV_{aggr}.

Dynamic light scattering (DLS) is a powerful technique used to determine the size of macromolecules and aggregates in the solution. In the present study we used DLS in order to characterise products formed as the results of incubation of the protein. The obtained graphs of size distribution estimated from the intensity percentage after a heating time of 72 h are shown in Fig. 6.

The DLS measurements for highly polydisperse samples are difficult and give rather qualitative information. Furthermore, for all samples, except for pure unheated lysozyme and lysozyme in 400 mM TMAO, the count rate plots presenting the number of photons detected per second were frequently disrupted by sharp spikes. These peaks originate from the large particle and since the DLS is not suitable for this type of measurements, these runs were removed from the calculation by a dust filtration algorithm [35].

In spite of the above-mentioned problems, it is still possible to draw some general conclusions. In the sample containing unheated lysozyme (Fig. 6A), the diameter of the detected macromolecules was equal to approximately 4 nm, which is in good agreement with data for native HEWL [7]. Samples with 0 mM TMAO of pH = 2 incubated at 60 °C for 72 h show a distinctive pattern in which the products of degradation, the intact lysozyme and aggregates with a diameter of around 300 nm are visible. The results for reaction mixtures containing 50 and 250 mM TMAO are in essence similar (for 250 mM TMAO the additional fraction was detected at around 50–60 nm but the degradation fragments are absent). Low precision and displacement of the peaks are caused by the rich composition of the solutions.

As with the other experimental techniques, the 400 mM TMAO sample gave a different pattern. First, unlike the other systems the obtained results are more repeatable and the measurements are stable. As was mentioned, the count rate plots for 400 mM TMAO are free of spikes and thus the number of large aggregates is reduced. After 12 h of heating the size distribution plots are well defined and change very little with incubation time. In contrast to

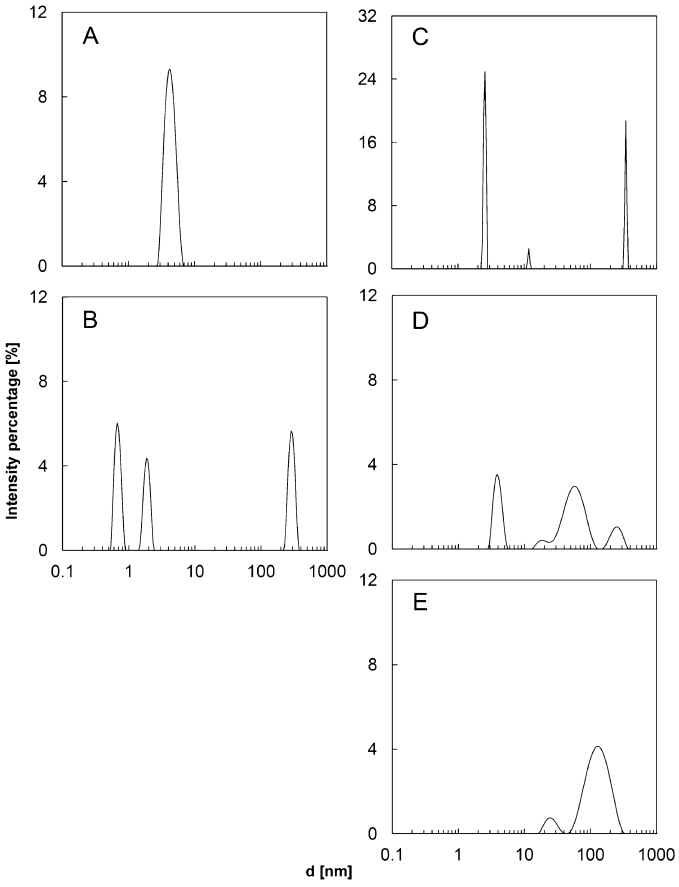

Fig. 6. Size distribution by intensity: (A) native HEWL without heating 0 mM TMAO; samples incubated at 60 °C for 72 h: (B) 0 mM TMAO; (C) 50 mM TMAO; (D) 250 mM TMAO; (E) 400 mM TMAO.

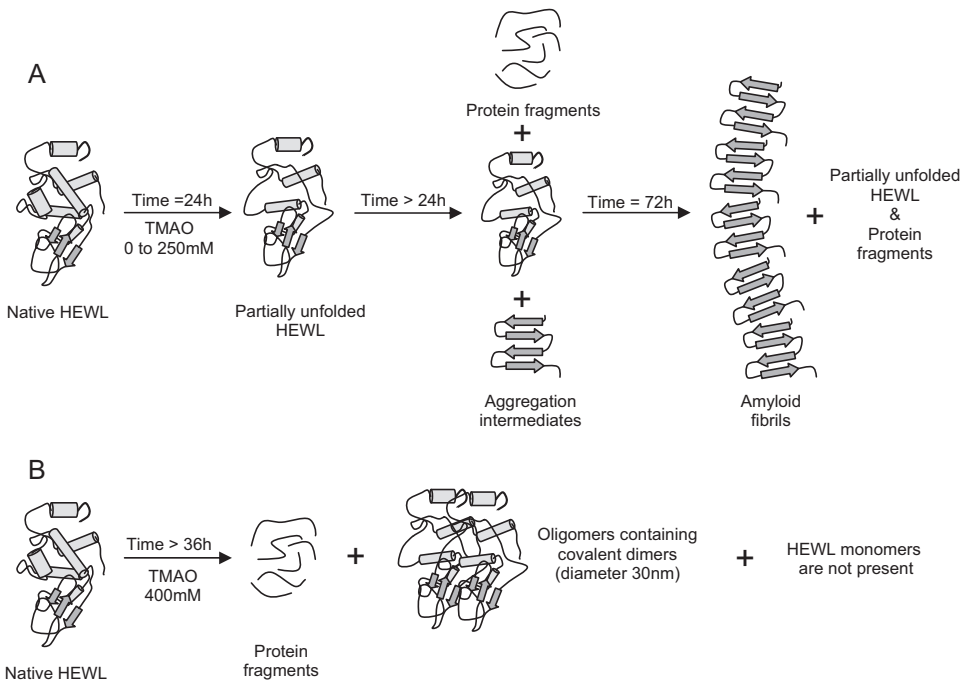

Fig. 7. Schematic illustration of the effects of trimethylamine N-oxide on the HEWL fibrillation (A) low concentration of TMAO and (B) 400 mM of TMAO.

other systems in the sample containing 400 mM TMAO, monomeric HEWL is absent.

Additional information can be obtained from the number distribution. As is widely known, the intensity of the scattered light is proportional to the diameter of the molecules to the power of 6. In other words, the larger the aggregate is, the scattering is more effective. Consequently, a small number of large particles will cause a significant scatter which will be noticeable on the plot of the size distribution by intensity. In the conditions of the present experiment, i.e. at the early stage of amyloidogenesis, the amount of formed aggregates is relatively small. As a result, in every sample except 400 mM TMAO the number distribution is overwhelmed by the presence of protein monomers (or protein fragments) and there is no indication of large particles on the graph of the size distribution by number (data not shown). In the sample where the concentration of trimethylamine N-oxide is the highest, practically a single fraction of clusters with a diameter of around 30 nm was detected. The similarity of plots for 250 and 400 mM of TMAO (Fig. 6D and E) is only illusive and this undeniable difference can be seen in the plots of size distribution by number.

4. Conclusions

The literature review of the impact of osmolytes on the fibrillation of protein as presented in the inspiring work of Macchi et al. [3] showed that the effects of these compounds on amyloidogenesis are, generally speaking, diversified, but in many instances weak. The present work revealed that the high concentration of the protonated form of trimethylamine N-oxide affects aggregation to a great degree. The influence of the reaction conditions on the protein structure and assembly is schematically summarised in Fig. 7.

According to our circular dichroism measurements, the lag time for acidic solution with a low concentration of TMAO is around 24 h. During this period the lysozyme unfolds but the content of the β-sheet remains constant. In contrast to the other samples, for 400 mM of TMAO there is no increase in the β-sheet fraction after 24 h of incubation. The protein undergoes irreversible denaturation but amyloids are not formed.

The atomic force microscopy scans suggest that the addition of TMAO changes the structure of the assembled fibrils. In the absence of TMAO the amyloids have a characteristic wavy shape, while for samples with 250 mM TMAO the formed amyloids are much shorter and straight. Furthermore, it is highly probable that before the amyloids can be detected by AFM, intermediates with a pronounced β-structure are created. There are no fibrils in the sample where the concentration of TMAO is 400 mM.

The plot of a specific volume (V_s) of HEWL versus incubation time (Fig. 5) also confirms the unique properties of systems containing 400 mM TMAO. In this case the V_s slightly increased due to protein degradation, and since fibrillation did not occur the decrease in V_s was not observed. However, aggregation of the protein was not completely avoided. SDS-PAGE electrophoresis demonstrated that, contrary to the rest of the systems, the dimerisation of HEWL with the formation of covalent bonds occurred. What is more, the dynamic light scattering measurements done for samples heated for 72 h showed that in the solution of lysozyme in 400 mM TMAO, clusters with a diameter of around 30 nm were present and that the analysed sample was exceptionally homogeneous. In this system no monomeric native-like HEWL was present. Samples where the concentration of TMAO was lower contained the degradation products of HEWL, the intact lysozyme and aggregates.

The mechanism of amyloid fibril formation is, in the classical approach, divided into three steps [17]: (a) partial unfolding of the protein, (b) formation of the intermediates/nucleation, and (c) elongation of the fibrils. Our studies prove that trimethylamine N-oxide in acidic solution inhibits amyloidogenesis after the first stage, i.e. protein unfolding. Incubation of hen egg white lysozyme (25 mg/ml) for 72 h at 60 °C in a solution of 400 mM of protonated TMAO (pH = 2) does not lead to the formation of amyloids. In these conditions TMAO inhibits amyloidogenesis but HEWL forms well-defined oligomeric aggregates.

Acknowledgement

This work was supported by the Faculty of Chemistry at Gdańsk University of Technology (mini-grant 030367).

References

[1] L.N. Arnaudov, R. de Vries, Biophys. J. 88 (2005) 515–526.
[2] F. Chiti, C.M. Dobson, Annu. Rev. Biochem. 75 (2006) 333–366.
[3] F. Macchi, M. Eisenkolb, H. Kiefer, D.E. Otzen, Int. J. Mol. Sci. 13 (2012) 3801–3819.
[4] S. Ghosh, N.K. Pandey, S. Bhattacharya, A. Roy, S. Dasgupta, Int. J. Biol. Macromol. 51 (2012) 1–6.
[5] K. Sasahara, H. Yagi, H. Naiki, Y. Goto, J. Mol. Biol. 372 (2007) 981–991.
[6] H.R. Kalhor, M. Kamizi, J. Akbari, A. Heydari, Biomacromolecules 10 (2009) 2468–2475.
[7] S.S.S. Wang, Y.-T. Hung, W.-S. Wen, K.-C. Lin, G.-Y. Chen, Biochim. Biophys. Acta 1811 (2011) 301–313.
[8] J.M. Khan, S.K. Chaturvedi, S.K. Rahman, M. Ishtikhar, A. Qadeer, E. Ahmada, R.H. Khan, Soft Matter 10 (2014) 2591–2599.
[9] S.S.S. Wang, Y.T. Hung, P. Wang, J.W. Wu, Korean J. Chem. Eng. 24 (2007) 787–795.
[10] B.A. Vernaglia, J. Huang, E.D. Clark, Biomacromolecules 5 (2004) 1362–1370.
[11] B.R. Zhou, Z. Zhou, Q.L. Hu, J. Chen, Y. Liang, Biochim. Biophys. Acta 1784 (2008) 472–480.
[12] S. Bahramikia, R. Yazdanparast, Int. J. Biol. Macromol. 50 (2012) 187–197.
[13] Z. Gazova, A. Bellova, Z. Daxnerova, J. Imrich, P. Kristian, J. Tomascikova, J. Bagelova, D. Fedunova, M. Antalik, Eur. Biophys. J. 37 (2008) 1261–1270.
[14] J. Krakowiak, J. Wawer, A. Panuszko, J. Chem. Thermodyn. 60 (2013) 179–190.
[15] P. Bruzdziak, P. Rakowska, J. Stangret, Appl. Spectrosc. 66 (2012) 1302–1310.
[16] P. Bruździak, A. Panuszko, J. Stangret, J. Phys. Chem. B 117 (2013) 11502–11508.
[17] T. Härd, C. Lendel, J. Mol. Biol. 421 (2012) 441–465.
[18] S.H. Khan, N. Ahmad, F. Ahmad, R. Kumar, IUBMB Life 62 (2010) 891–895.
[19] V. Granata, P. Palladino, B. Tizzano, A. Negro, R. Berisio, A. Zagari, Biopolymers 82 (2006) 234–240.
[20] R. Singh, I. Haque, F. Ahmad, J. Biol. Chem. 280 (2005) 11035–11042.
[21] L. Whitmore, B.A. Wallace, Nucleic Acids Res. 32 (2004) W668–W673.
[22] L. Whitmore, B.A. Wallace, Biopolymers 89 (2008) 392–400.
[23] M.A. Andrade, P. Chacon, J.J. Merelo, F. Moran, Protein Eng. 6 (1993) 383–390.
[24] S.E. Hill, T. Miti, T. Richmond, M. Muschol, PLoS ONE 6 (2011) e18171.
[25] M. Bartolini, C. Bertucci, M.L. Bolognesi, A. Cavalli, C. Melchiorre, V. Andrisano, ChemBioChem 8 (2007) 2152–2161.
[26] B. Maroufi, B. Ranjbar, K. Khajeh, H. Naderi-Manesh, H. Yaghoubi, Biochim. Biophys. Acta 1784 (2008) 1043–1049.
[27] B.L. Simons, M.C. King, T. Cyr, M.A. Hefford, H. Kaplan, Protein Sci. 11 (2002) 1558–1564.
[28] Y. Desfougères, J. Jardin, V. Lechevalier, S. Pezennec, F. Nau, Biomacromolecules 12 (2011) 156–166.
[29] J. Xie, M. Qin, Y. Cao, W. Wang, Proteins 79 (2011) 2505–2516.
[30] K. Sasahara, M. Sakurai, K. Nitta, J. Mol. Biol. 291 (1999) 693–701.
[31] V.A. Sirotkin, R. Winter, J. Phys. Chem. B 114 (2010) 16881–16886.
[32] L. Mitra, J.-B. Rouget, B. Garcia-Moreno, C.A. Royer, R. Winter, ChemPhysChem 9 (2008) 2715–2721.
[33] V. Smirnovas, R. Winter, T. Funck, W. Dzwolak, ChemPhysChem 7 (2006) 1046–1049.
[34] K. Akasaka, A.R.A. Latif, A. Nakamura, K. Matsuo, H. Tachibana, K. Gekko, Biochemistry 46 (2007) 10444–10450.
[35] Zetasizer Nano: User Manual, Malvern Instruments Ltd., Worcestershire, 2007 (Issue 3.1).